BIULETYN PAŃSTWOWEGO INSTYTUTU GEOLOGICZNEGO 474: 73–84, 2019 R.
DOI: 10.5604/01.3001.0013.0826

THE CHARACTERISTICS OF PORE SPACE IN LOWER TRIASSIC SANDSTONES OF THE WARSAW REGION

CHARAKTERYSTYKA PRZESTRZENI POROWEJ PIASKOWCÓW TRIASU DOLNEGO OKOLIC WARSZAWY

Marta Kuberska[1], Anna Becker[1], Aleksandra Kozłowska[1]

Abstract. Reservoir and sealing properties of Lower Triassic sandstones from seven boreholes of the central part of the Koszalin-Zamość Synclinorium were investigated in terms of potential levels for underground storage of carbon dioxide. Extensive petrographic studies, image analysis, and investigations of petrophysical properties of rocks and pore space were carried out. The research shows that diagenetic processes both variously affected the intensity of alteration and variously shaped the pore space. Not only primary but also secondary porosity, resulting from diagenetic alteration and dissolution, is observed in the rocks. Microscopic observations revealed that the pore space in studied samples is dominated by macropores. The results obtained indicate a poor suitability of the Lower Triassic deposits for the purpose of carbon dioxide sequestration.

Key words: the pore space of sandstones, the Lower Triassic, the Warsaw region.

Abstrakt. W pracy przedstawiono badania piaskowców triasu dolnego centralnej części synklinorium koszalińsko-zamojskiego pochodzących z siedmiu otworów wiertniczych, pod kątem ich właściwości kolektorsko-uszczelniających w aspekcie potencjalnych poziomów do podziemnego składowania dwutlenku węgla. Przeprowadzono szeroko zakrojone badania petrograficzne, analizę obrazu i badania właściwości petrofizycznych skał oraz przestrzeni porowej. W wyniku przeprowadzonych prac stwierdzono, że procesy diagenetyczne miały różny wpływ na intensywność zmian i w różny sposób kształtowały przestrzeń porową. W skałach zaobserwowano występowanie porowatości pierwotnej, a także wtórnej, powstałej na skutek przeobrażania i rozpuszczania diagenetycznego. Na podstawie obserwacji mikroskopowych uznano, że przestrzeń porowa w badanych próbkach jest zdominowana przez makropory. Wyniki badań wskazują na niewielką przydatność utworów triasu dolnego na potrzeby sekwestracji dwutlenku węgla.

Słowa kluczowe: przestrzeń porowa piaskowców, trias dolny, okolice Warszawy.

INTRODUCTION

Lower Triassic rocks from the central part of the Koszalin-Zamość Synclinorium (borderland of the Warsaw and Puławy segments – Żelaźniewicz *et al*., 2011; Aleksandrowski, 2017) were investigated for their reservoir properties, as potential levels for underground storage of carbon dioxide (Wójcicki, 2013). From this point of view, the most interesting rock successions are those located above the depth of 2500 m, which is considered a depth limit for possible carbon dioxide storage in geologic structures, with the porosity and permeability not lower than 10% (optimal >20%) and 10 mD (optimal >300 mD, respectively) (Chadwick *et al*., 2006; Wójcicki, 2013). Petrographic studies were performed on sandstone samples from the following boreholes: Białobrzegi IG 1 (2159.0–2405.2 m), Gradzanowo 2 (2413.0–2866.0 m), Maciejowice IG 1 (1600.0–1765.0 m), Magnuszew IG 1 (1810.0–1976.5 m), Nadarzyn IG 1 (2523.0–2811.0 m), Warka IG 1 (2047.5–2259.5 m), Wilga IG 1 (1887.5–2034.5 m).

[1] Polish Geological Institute – National Research Institute, 4 Rakowiecka Street, 00-975 Warsaw, Poland; e-mail: marta.kuberska@pgi.gov.pl, anna.becker@pgi.gov.pl, aleksandra.kozlowska@pgi.gov.pl.

RESEARCH METHODS

Microscopic examinations of thin sections were carried out using a Nikon Optiphot 2 polarizing microscope. The mineral percentage of the sandstone samples was the object of the estimations under the microscope, the modified nomenclature after Pettijohn *et al*. (1972) being applied. All minerals were subjected to dye analysis to identify carbonates (Migaszewski, Narkiewicz, 1983). Cathodoluminescence (CL) studies were also performed using an equipment with a CITL Mk5-2 cold cathode. Cathodoluminescence observations were helpful in identifying cement types (quartz, kaolinite and carbonates) as well as in the examinations of detrital grains. Research on microstructures of rocks and morphology of minerals, and observations of pore space development were made in Polish Geological Institute – National Research Institute (PGI-NRI) using a LEO 1430 scanning electron microscope coupled with the X-ray microanalyzer with energy dispersion, which enabled chemical analyses in selected micro-areas. The computer image analysis was performed on preparations stained with blue resin, using a Nikon Eclipse E600 polarizing microscope coupled with the computer equipped with the Lucia image analysis software, which enabled to identify parameters characterising the pore space (*e.g.*, diameter, perimeter, mean chord, length, width) and described in the papers by Leśniak (1999) and Kozłowska, Kuberska (2006).

GEOLOGICAL SETTING

In the Mesozoic structural pattern, the study area is located in the central part of the Koszalin-Zamość Synclinorium, fringing the Mid-Polish Anticlinorium from the north east (Fig. 1). According to Żelaźniewicz *et al*. (2011) this synclinal structure can be subdivided into segments, of which the Warsaw segment covers its central part formerly called the Warsaw or Płock Trough (*e.g.*, Marek, 1983; Narkiewicz, Dadlez, 2008). The Lower Triassic deposits in the study area are typical of the eastern part of the central European Basin, in which terrestrial-marine deposits of very shallow environments were accumulated in the Early Triassic under arid climate conditions (see *e.g.*, Szyperko-Teller *et al*., 1997; Becker, 2019a, b). The Lower Triassic succession is dominated by red-brown massive or laminated claystones and mudstones with sandstone interbeds (Fig. 2). In the lower part of the

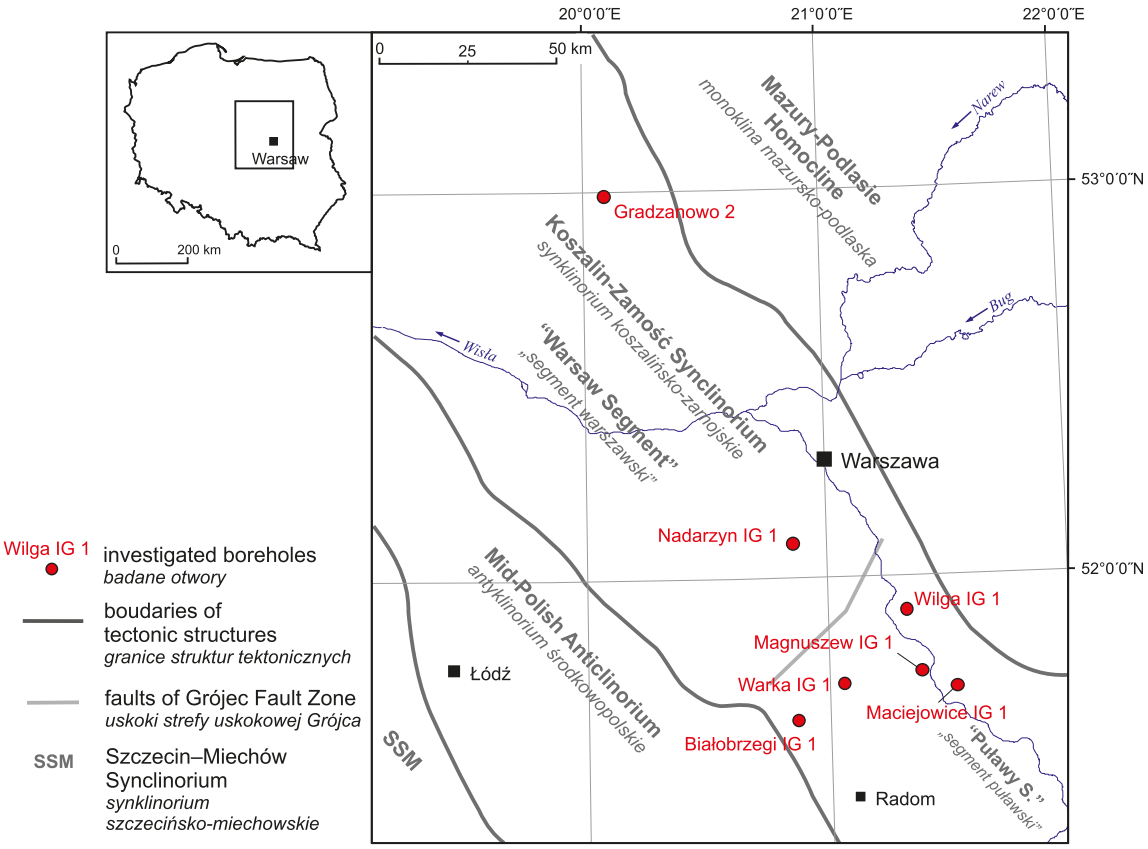

Fig. 1. Localization of studied boreholes against tectonic structures of the pre-Cenozoic realm (after Aleksandrowski, 2017). Segments of the Koszalin-Zamość Synklinorium adopted from Żelaźniewicz *et al*. (2011)

Lokalizacja badanych otworów na tle struktur tektonicznych planu podkenozoicznego (wg Aleksandrowskiego, 2017). Podział synklinorium koszalińsko-zamojskiego na segmenty przyjęto za Żelaźniewiczem i in. (2011)

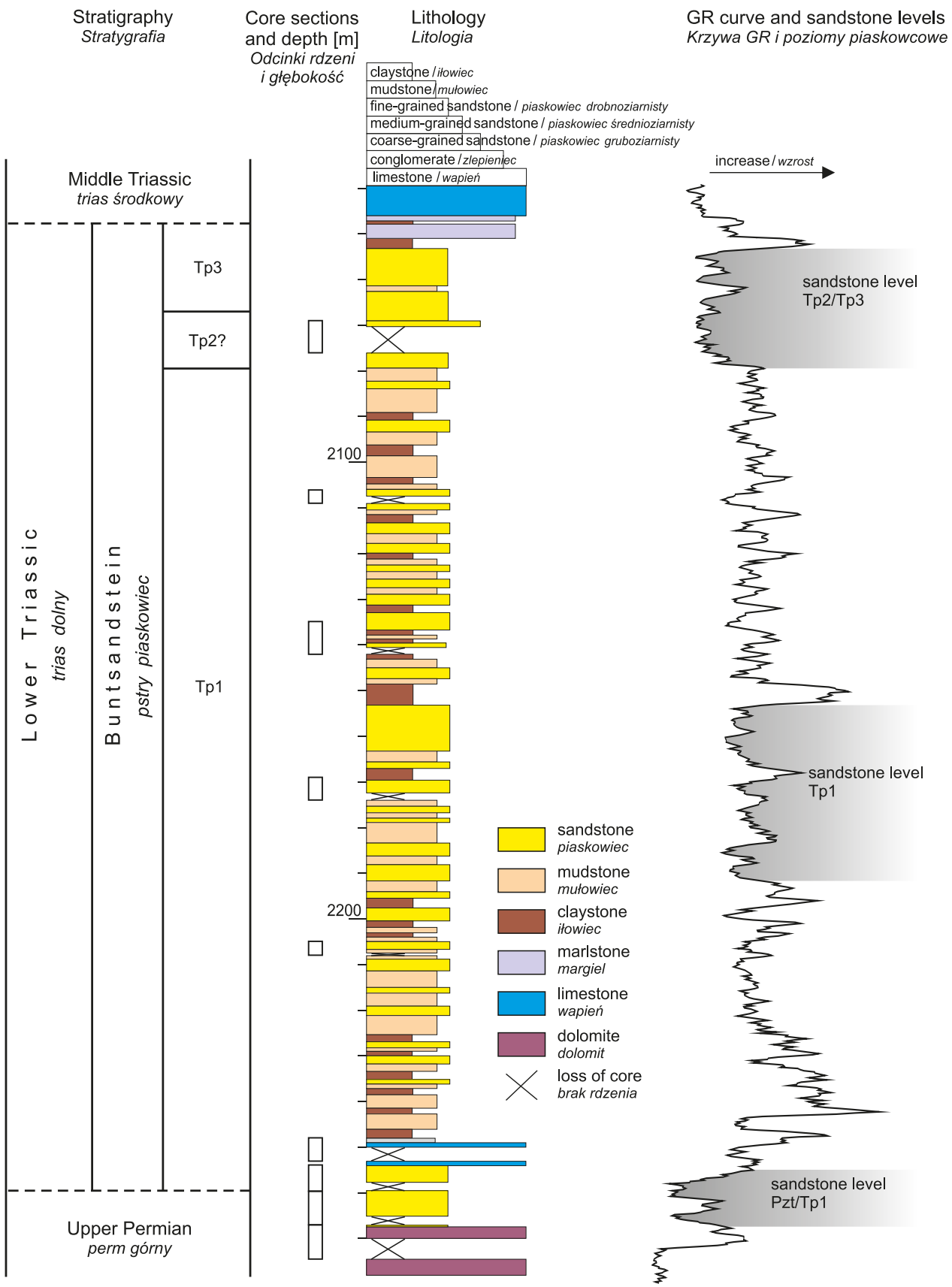

Fig. 2. Example of Buntsandstein lithologic section in the Warka IG 1 borehole (lithology after A. Becker, stratigraphy after Szyperko-Śliwczyńska, 1980, modified)

Przykładowy profil litologiczny pstrego piaskowca dla otworu wiertniczego Warka IG 1 (litologia wg A. Becker, stratygrafia wg Szyperko-Śliwczyńskiej, 1980, zmodyfikowane)

succession (Lower Buntsandstein), these interbeds form thin layers, several cm in thickness, whereas in the upper part (Middle and Upper Buntsandstein) – complexes up to 50-m thick. Within such complexes, sandstones can pass into calcareous sandstones or even sandy limestones. There are also subordinate interbeds of claystones and mudstones. Very thin limestone interbeds are found in the lower part of the succession mainly in the northern part of the study area (Nadarzyn IG 1 and Gradzanowo 2 boreholes). The thickness of the Lower Triassic varies from 147.0 m in the Wilga IG 1 borehole to 453.0 m in the Gradzanowo 2 borehole, and is typical of areas located outside the basin depocentre. Nevertheless, the sediment deposition rate in this area was very high in the Early Triassic (Dyrka, 2018). The greatest depth to the top of the Lower Triassic is reported from the northern part of the area. In the Gradzanowo 2 borehole, it occurs just above the limit depth of 2500 m. This horizon gradually descends towards the east and southeast (*cf.* Bachmann *et al*., 2010). In the Maciejowice IG 1 borehole it was found at the depth of 1600 m (depths after CBDG, 2008). Five sandstone-dominated horizons have been identified within the Lower Triassic succession and analysed for reservoir properties. These occur (Fig. 2) (1) at the uppermost Permian/lowermost Triassic boundary, mainly in the southern part of the study area, (2) in the mid-Lower Buntsandstein, (3) in the lowermost Middle Buntsandstein, (4) in the mid-Middle Buntsandstein, and (5) in the lower Upper Buntsandstein. In the Warsaw region and southwest of Warka, the two latter horizons can merge into one single sandstone horizon.

RESEARCH RESULTS

RESULTS OF PETROGRAPHIC STUDIES OF SANDSTONES

The sandstones are characterized by a psammitic structure, locally psammitic-aleuritic, and unoriented texture. They are poorly sorted and very poorly coherent. A better packing of detrital material is observed only locally. The rocks occur mainly as variously thick packets among claystones and mudstones. They represent arenites; some are quartz and subarkosic wackes, sporadically sublithic. Most of the sandstones are fine-grained varieties, and the average diameter of detrital grains ranges from about 0.12 to 0.18 mm. The main detrital components are subrounded monocrystalline quartz crystals. Feldspars are represented mainly by potassium varieties, rarely plagioclases. Sublithic varieties are enriched in magmatic and sedimentary lithoclasts. Micas in small amounts have been also observed. Some of them display the effects of chlorization process. Detrital material is cemented by matrix and orthochemical cement. The matrix is a mixture of detrital clay minerals, iron compounds and, locally, mud, while the cement is composed of carbonates (Fig. 3A–D, dolomite, calcite, ankerite), occasionally of authigenic quartz (Fig. 3D), and sporadically of anhydrite. There are also small concentrations of kaolinite and chlorites. Small amounts of calcite represented by anhedral individuals have been found in sandstones. Dolomite occurs as variously sized rhombohedrons. In CL, it shows red-brown to dark brown colours and a characteristic zonal structure. The zones of very dark luminescence, and thus probably enriched with iron, may have the composition of ankerite. Ankerite rhombohedra with thin ankerite rims were also identified (Fig. 3C). The amount of quartz cement is low; it forms regeneration rims on detrital grains. Kaolinite is represented by platy aggregates, filling the pore spaces, or creates fillings within detrital grains. Kaolinite plates occur as so-called vermicular or irregular forms. In the examined sandstones, the trace amounts of fibrous illite were recorded.

RESULTS OF COMPUTER IMAGE ANALYSIS

Microscopic image analysis comprised seven sandstone samples providing information on the actual size of pores in the rock, and on their shape and distribution. The selected and measured parameters are shown statistically in Table 1. The porosity of sandstones in these samples ranges from 2.30 (Gradzanowo 2) to 16.33 vol.% (Nadarzyn IG 1). The pores that are 0.01–0.04 mm in length and width account for about 90% (Tab. 2) in the samples. The pores with the minimum and maximum Feret diameter, equivalent diameter, and average pore chords in the range 0.01–0.04 mm constitute more than 80% of all pores. The pores with the equivalent sphere and cylinder size below 0.001 mm make up almost 100%. The most varying parameter is the perimeter of the pore spaces. Their largest percentage falls in the range of 0.01–0.05 mm. The pores ranging in size 0.5–1.0 mm are characterized by the maximum circularity, the parameter that determines the surface of the tested object in relation to an ideal circle (Leśniak, 1999). On the other hand, over 99% of pores larger than 1 mm in size exhibit elongation, which is the ratio of the maximum and minimum Feret diameter.

CHARACTERISTICS OF PETROPHYSICAL PROPERTIES AND PORE SPACE OF THE SANDSTONES

We can observe the effects of mechanical compaction (intergranular point and straight contacts), cementation (carbonates, authigenic quartz, kaolinite), dissolution and diagenetic alteration (secondary inter- and intragranular porosity and inter-crystalline porosity). These processes variously affected the persistence of primary porosity or the formation of secondary porosity in the sediment (Fig. 4A–F). Secondary porosity was mainly observed in subarkosic varieties, where diagenetic dissolution of feldspars occurred (Fig. 4A, B).The effects of diagenetic dissolution of components in cements were also noticed (Fig. 4C–F).

As it is presented by Wójcicki *et al*. (2014) in the sandstones from the Warka IG 1 borehole the total porosity varies from 16.58 to 30.71%. Considerable differences in the hysteresis values, ranging between 11 and 70%, indicate a relatively chaotic development of pore space. In most of the samples, the percentage of pores > 1 μm is more than

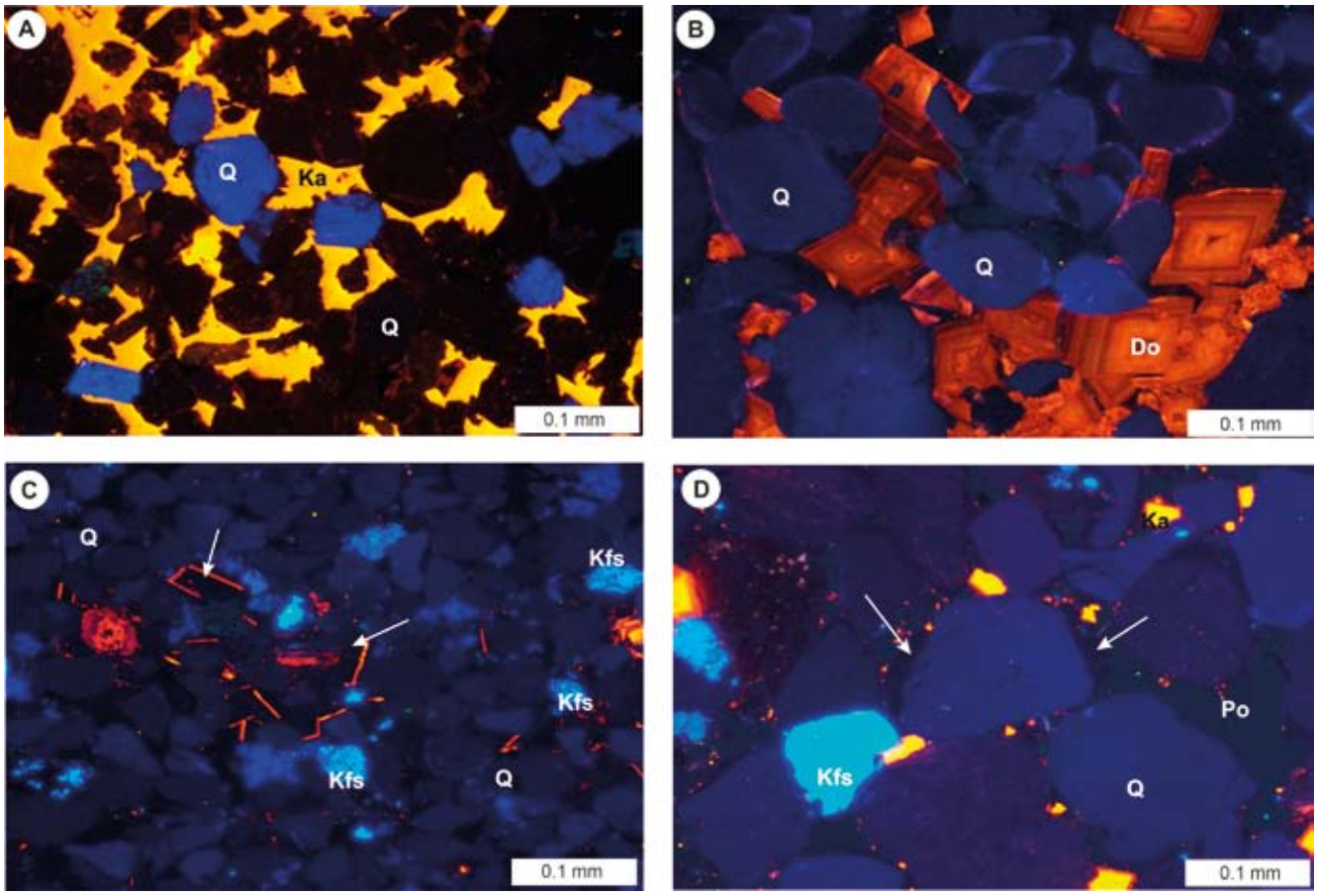

Fig. 3. Cathodoluminescence (CL) microphotographs

A – fragment of sandstone with calcite cement (Ka; yellow luminescence), quartz grains (Q) with blue and brown luminescence, Nadarzyn IG 1 borehole, depth 2663.1 m; **B** – fragment of sandstone, quartz grains (Q), dolomite rhombohedra (Do) of zonal structure, Wilga IG 1 borehole, depth 1896.4 m; **C** – fragment of sandstone, quartz grains (Q), potassium felspars (Kfs), ankerite rhombohedra (arrows) with thin dolomite rims, Warka IG 1 borehole, depth 2259.5 m; **D** – fragment of sandstone of composition of quartz arenite, quartz grains (Q), potassium feldspars (Kfs) and calcite (Ka), authigenic quartz overgrowths (arrows) on quartz grains, primary porosity (Po) preserved between grains, Nadarzyn IG 1 borehole, depth 2602.1 m

Obrazy mikroskopowe w katodoluminescencji

A – fragment piaskowca o spoiwie kalcytowym (Ka; luminescencja w barwach żółtych), widoczne ziarna kwarcu (Q) o niebieskiej i brunatnej luminescencji, otwór Nadarzyn IG 1, głęb. 2663,1 m; **B** – fragment piaskowca, widoczne ziarna kwarcu (Q) oraz romboedry dolomitu (Do) o budowie pasowej, otwór Wilga IG 1, głęb. 1896,4 m; **C** – fragment piaskowca, widoczne ziarna kwarcu (Q), skaleni potasowych (Kfs) oraz romboedry ankerytu (strzałki) z cienkimi dolomitowymi obwódkami, otwór Warka IG 1, głęb. 2259,5 m; **D** – fragment piaskowca o składzie arenitu kwarcowego, widoczne ziarna kwarcu (Q) i skaleni potasowych (Kfs) oraz kalcyt (Ka), na ziarnach kwarcu widoczne narastające autigeniczne kwarcowe obwódki (strzałki), a między ziarnami zachowana porowatość pierwotna (Po); otwór Nadarzyn IG 1, głęb. 2602,1 m

80%. In one sample from the Wilga IG 1 borehole (depth 1896.4 m) the total porosity is 12.64%, and from the Gradzanowo 2 borehole (sample from 2481.1 m depth) – it reaches 17.43%. In these samples the hysteresis effect falls within the limits of 62–65%, and the pores > 1 μm account for 58% of the total.

The effective porosities given in boreholes' final reports are summarised in Table 3. The maximum average values of effective porosity were reported for sandstones from the Wilga IG 1 and Maciejowice IG 1 boreholes. The permeability measured in these samples is highly variable and ranges from several mD to a few hundred mD.

CONCLUSIONS

Petrophysical properties of the Triassic sandstones are shaped by very different factors. Significant ones include diagenetic processes proceeding in the sediment after its deposition (compare: Kuberska, 1997, 1999). In these sandstones, the effects of the following processes have been noticed: weak mechanical compaction, cementation (authigenic quartz, calcite, dolomite/ankerite?, anhydrite, kaolinite, chlorite), replacement, and diagenetic dissolution and alteration. Cementation has led to the formation of fringe, pore and, locally, base cements. Carbonate cements were most

Table 1

Statistical results of the computer image analysis of pore space and sandstone porosity

Statystyczne wyniki komputerowej analizy obrazu mikroskopowego przestrzeni porowej i porowatość piaskowców

Borehole	Depth	Eq diameter	Perimeter	Mean chord	Length	Width	Max Feret	Min Feret	Circularity	Elongation	Porosity
	[m]	[mm]									[%]
Białobrzegi IG 1	2185.5	0.01	0.04	0.01	0.02	0.01	0.01	0.01	0.73	1.63	3.68
		0.01	0.05	0.01	0.02	0.005	0.02	0.01	0.213	0.49	
		0.0005	0.001	0.0006	0.0005	0.0005	0.0005	0.0005	0.097	1	
		0.1	0.5	0.05	0.22	0.05	0.17	0.08	1	6.01	
Gradzanowo 2	2483.5	0.01	0.03	0.005	0.01	0.004	0.01	0.01	0.759	1.66	2.30
		0.01	0.03	0.004	0.01	0.003	0.01	0.01	0.212	0.53	
		0.0005	0.001	0.0006	0.0005	0.0005	0.0005	0.0005	0.109	1	
		0.06	0.39	0.03	0.18	0.03	0.09	0.07	1	7.17	
Magnuszew IG 1	1973.4	0.01	0.04	0.01	0.01	0.005	0.01	0.01	0.751	1.68	7.28
		0.01	0.05	0.01	0.02	0.005	0.02	0.01	0.209	0.62	
		0.0005	0.001	0.0006	0.0005	0.0005	0.0005	0.0005	0.129	1	
		0.25	1.24	0.12	0.53	0.09	0.34	0.23	1	13.65	
Nadarzyn IG 1	2602.1	0.01	0.05	0.01	0.02	0.01	0.02	0.01	0.748	1.78	16.33
		0.02	0.08	0.01	0.03	0.01	0.03	0.02	0.237	0.97	
		0.0005	0.001	0.0006	0.0005	0.0005	0.0005	0.0005	0.069	1	
		0.24	1.28	0.12	0.59	0.09	0.34	0.23	1	14.32	
Warka IG 1	2069.2	0.01	0.04	0.01	0.02	0.01	0.01	0.01	0.731	1.61	12.32
		0.01	0.05	0.01	0.02	0.01	0.02	0.01	0.221	0.56	
		0.0005	0.001	0.0006	0.0005	0.0005	0.0005	0.0005	0.085	1	
		0.12	0.69	0.07	0.32	0.06	0.17	0.13	1	20.5	
Warka IG 1	2259.1	0.01	0.03	0.004	0.01	0.003	0.01	0.01	0.757	1.65	6.43
		0.01	0.03	0.003	0.01	0.002	0.01	0.01	0.226	0.54	
		0.0005	0.001	0.0006	0.0005	0.0005	0.0005	0.0005	0.107	1	
		0.06	0.32	0.02	0.14	0.02	0.09	0.05	1	10.61	
Wilga IG 1	1912.8	0.01	0.03	0.004	0.01	0.003	0.01	0.01	0.749	1.71	7.44
		0.01	0.03	0.003	0.01	0.002	0.01	0.01	0.243	0.74	
		0.0005	0.001	0.0006	0.0005	0.0005	0.0005	0.0005	0.065	1	
		0.11	0.54	0.05	0.23	0.04	0.15	0.1	1	18.73	

mean / średnia
standard deviation / odchylenie standardowe
minimum
maximum

often sealing the sandstone pores. The forms and type of clay minerals had a various effect on the petrophysical properties of the sandstones (compare: Kuberska, 1997, 1999). For example, book-like kaolinite in the pore spaces closed the pores, limiting the permeability capacity of the rocks. On the other hand, blocky kaolinite or its single crystallites, loosely distributed in the pores, did not affect the permeability properties so restrictively. The presence of fibrous illite had a negative effect in this respect; however, it does not occur frequently in the sandstones examined. The sediment permeability can also be limited by chlorites, depending on their mode of occurrence. It is believed, however, that this limitation occurs only to a small extent due to the low ability of chlorites to adsorb fluids (Plewa M., Plewa S., 1992).

Diagenetic processes both variously affected the intensity of alterations and variously shaped the pore space. Therefore, primary and secondary porosity resulting from diagenetic alteration and dissolution is noticed.

Microscopic observations indicate that the pore space in the samples examined is dominated by macropores. As it results from the size of micropores, the pores that are 0.01–0.04 mm in length and width account for about 90% in the samples (Tab. 2). That is why, the Triassic sandstones here described show reservoir properties that only selectively and at certain points meet the petrophysical criteria for suitability as storage sites in carbon dioxide sequestration. Exhibiting generally sufficient porosities, these deposits often show unadequate permeability, as found also for the Upper Triassic rocks of northern Mazovia (Feldman-Olszewska *et al*., 2012). An additional challenge is the variability of the analysed parameters. The use of Lower Triassic deposits would require very detailed research to identify rock bodies with uniform, favourable reservoir properties, suitable for local, probably small, storage facilities.

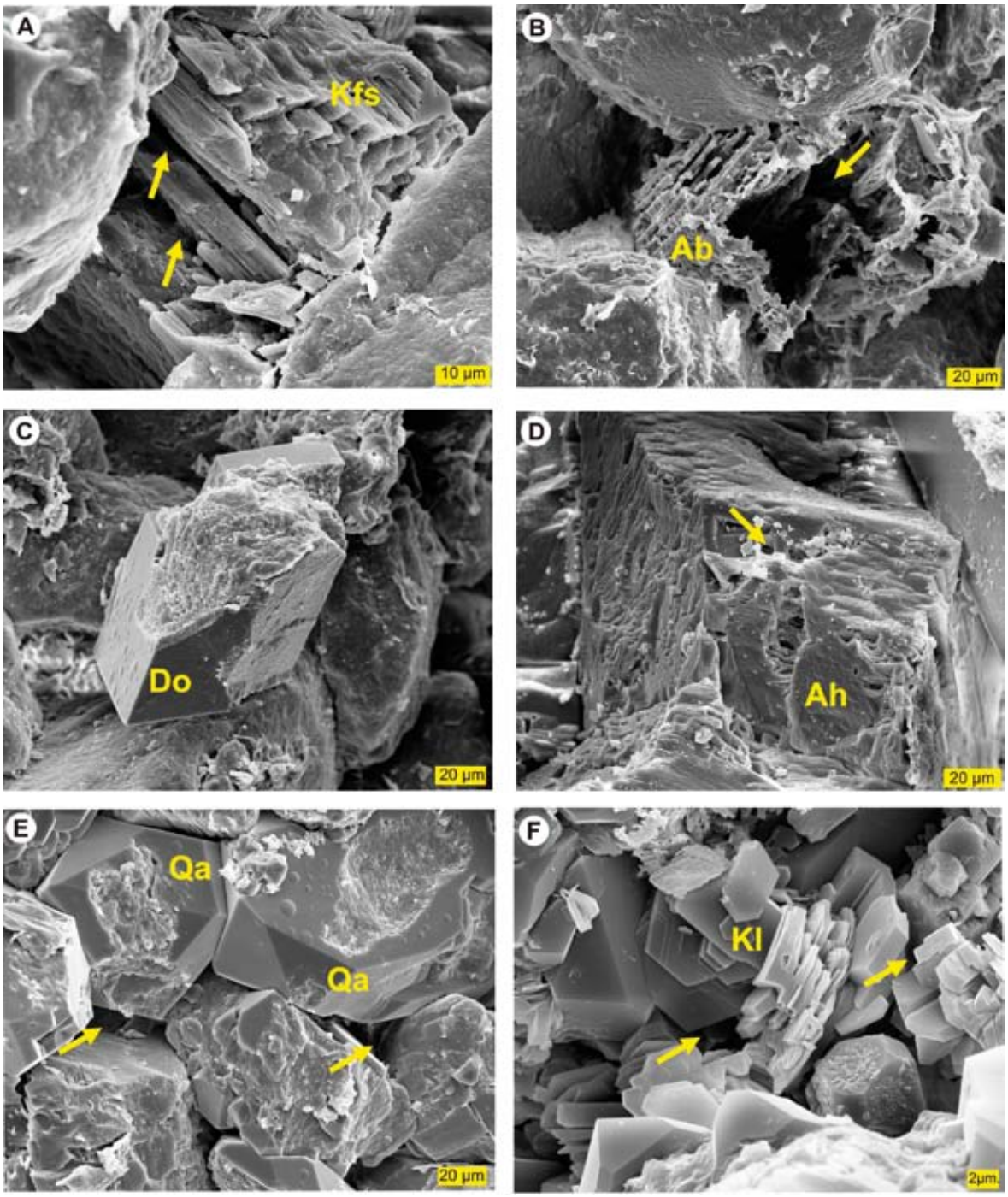

Fig. 4. SEM images (photographs by L. Giro)

A – potassium feldspar (Kfs) with traces of diagenetic dissolution (arrows), Białobrzegi IG 1 borehole, depth. 2184.1 m; **B** – albite relic (Ab) after its dissolution, secondary porosity (arrow) visible, Warka IG 1 borehole, depth 2207.1 m; **C** – partly dissolved dolomite crystal (Do) in porous space of sandstone, Magnuszew IG 1 borehole, depth 1973.4 m; **D** – anhydrite (Ah) with traces of diagenetic dissolution (arrow), Nadarzyn IG 1 borehole, depth 2602.1 m; **E** – quartz with traces of partial diagenetic dissolution and preserved primary porosity (arrows), Gradzanowo 2 borehole, depth 2483.5 m; **F** – porosity (arrows) between crystallinites of kaolinite (Kl), Warka IG 1 borehole, depth 2259.1 m

Obrazy z elektronowego mikroskopu skaningowego (fot. wyk. L. Giro)

A – skaleń potasowy (Kfs) z widocznymi śladami rozpuszczania diagenetycznego (strzałki), otwór Białobrzegi IG 1, głęb. 2184,1 m; **B** – relikt albitu (Ab) pozostały po jego rozpuszczeniu, widoczna wtórna porowatość (strzałka), otwór Warka IG 1, głęb. 2207,1 m; **C** – częściowo rozpuszczony kryształ dolomitu (Do) w przestrzeni porowej piaskowca, otwór Magnuszew IG 1, głęb. 1973,4 m; **D** – anhydryt (Ah) z widocznymi śladami rozpuszczania diagenetycznego (strzałka), otwór Nadarzyn IG 1, głęb. 2602,1 m; **E** – kwarc z widocznymi śladami częściowego rozpuszczania diagenetycznego oraz zachowana pierwotna mikroporowatość (strzałki), otwór Gradzanowo 2, głęb. 2483,5 m; **F** – porowatość (strzałki) między krystalitami kaolinitu (Kl), otwór Warka IG 1, głęb. 2259,1 m

Table 2

Pore space parameters in dependence of pore size

Parametry przestrzeni porowej w zależności od wielkości porów

Borehole and depth [m]	Parameters	Size ranges (intervals) [mm]																				
		0.001	0.01	0.02	0.03	0.04	0.05	0.06	0.07	0.08	0.09	0.1	0.12	0.14	0.16	0.2	0.3	0.4	0.5	0.6	1	>1
Białobrzegi IG 1 2185.5	Eq diameter	1.00	77.98	11.75	4.81	2.56	1.03	0.53	0.16	0.12	0.03	0.03	0.00	0.00	0.00	0.00	0.00	0.00	0.00	0.00	0.00	0.00
	Volume Eq Sphere	100.00	0.00	0.00	0.00	0.00	0.00	0.00	0.00	0.00	0.00	0.00	0.00	0.00	0.00	0.00	0.00	0.00	0.00	0.00	0.00	0.00
	Volume Eq Cylinder	100.00	0.00	0.00	0.00	0.00	0.00	0.00	0.00	0.00	0.00	0.00	0.00	0.00	0.00	0.00	0.00	0.00	0.00	0.00	0.00	0.00
	Perimeter	0.12	39.08	15.28	8.78	6.81	5.12	3.78	3.56	2.66	2.47	1.84	2.62	1.81	2.19	1.81	1.56	0.37	0.12	0.00	0.00	0.00
	Mean Chord	1.59	89.97	6.65	1.44	0.25	0.09	0.00	0.00	0.00	0.00	0.00	0.00	0.00	0.00	0.00	0.00	0.00	0.00	0.00	0.00	0.00
	Length	0.66	66.45	12.34	7.37	3.75	3.06	1.91	1.44	1.03	0.62	0.28	0.56	0.19	0.19	0.12	0.03	0.00	0.00	0.00	0.00	0.00
	Width	12.28	82.26	4.65	0.75	0.03	0.03	0.00	0.00	0.00	0.00	0.00	0.00	0.00	0.00	0.00	0.00	0.00	0.00	0.00	0.00	0.00
	Max Feret	0.66	66.98	13.71	7.97	4.15	2.97	1.62	0.94	0.37	0.19	0.12	0.22	0.06	0.00	0.03	0.00	0.00	0.00	0.00	0.00	0.00
	Min Feret	1.75	79.79	10.34	4.37	2.34	0.75	0.41	0.09	0.16	0.00	0.00	0.00	0.00	0.00	0.00	0.00	0.00	0.00	0.00	0.00	0.00
	Circularity	0.00	0.00	0.00	0.00	0.00	0.00	0.00	0.00	0.00	0.00	0.03	0.00	0.00	0.00	0.00	0.78	6.00	10.53	15.25	67.42	0.00
	Elongation	0.00	0.00	0.00	0.00	0.00	0.00	0.00	0.00	0.00	0.00	0.00	0.00	0.00	0.00	0.00	0.00	0.00	0.00	0.00	0.12	99.88
Gradzanowo 2 2483.5	Eq diameter	1.08	86.35	9.40	2.41	0.61	0.14	0.02	0.00	0.00	0.00	0.00	0.00	0.00	0.00	0.00	0.00	0.00	0.00	0.00	0.00	0.00
	Volume Eq Sphere	100.00	0.00	0.00	0.00	0.00	0.00	0.00	0.00	0.00	0.00	0.00	0.00	0.00	0.00	0.00	0.00	0.00	0.00	0.00	0.00	0.00
	Volume Eq Cylinder	100.00	0.00	0.00	0.00	0.00	0.00	0.00	0.00	0.00	0.00	0.00	0.00	0.00	0.00	0.00	0.00	0.00	0.00	0.00	0.00	0.00
	Perimeter	0.23	45.67	16.85	9.04	6.86	4.60	4.04	3.04	2.10	1.94	1.38	1.60	1.19	0.52	0.72	0.18	0.04	0.00	0.00	0.00	0.00
	Mean Chord	1.83	95.74	2.34	0.09	0.00	0.00	0.00	0.00	0.00	0.00	0.00	0.00	0.00	0.00	0.00	0.00	0.00	0.00	0.00	0.00	0.00
	Length	0.50	75.12	11.07	6.43	2.93	1.72	1.06	0.52	0.32	0.14	0.05	0.05	0.05	0.00	0.02	0.00	0.00	0.00	0.00	0.00	0.00
	Width	12.43	86.54	1.01	0.02	0.00	0.00	0.00	0.00	0.00	0.00	0.00	0.00	0.00	0.00	0.00	0.00	0.00	0.00	0.00	0.00	0.00
	Max Feret	0.50	75.31	13.65	6.31	2.46	1.01	0.47	0.23	0.04	0.02	0.00	0.00	0.00	0.00	0.00	0.00	0.00	0.00	0.00	0.00	0.00
	Min Feret	1.80	87.96	7.62	1.99	0.45	0.09	0.05	0.04	0.00	0.00	0.00	0.00	0.00	0.00	0.00	0.00	0.00	0.00	0.00	0.00	0.00
	Circularity	0.00	0.00	0.00	0.00	0.00	0.00	0.00	0.00	0.00	0.00	0.00	0.02	0.00	0.00	0.04	1.01	4.44	9.63	11.75	73.12	0.00
	Elongation	0.00	0.00	0.00	0.00	0.00	0.00	0.00	0.00	0.00	0.00	0.00	0.00	0.00	0.00	0.00	0.00	0.00	0.00	0.00	0.23	99.77

Table 2 cont.

1	2	3	4	5	6	7	8	9	10	11	12	13	14	15	16	17	18	19	20	21	22	23
Magnuszew IG 1 1973.4	Eq diameter	0.74	82.90	9.98	3.52	1.49	0.63	0.27	0.21	0.10	0.04	0.04	0.04	0.00	0.00	0.02	0.01	0.00	0.00	0.00	0.00	0.00
	Volume Eq Sphere	99.97	0.03	0.00	0.00	0.00	0.00	0.00	0.00	0.00	0.00	0.00	0.00	0.00	0.00	0.00	0.00	0.00	0.00	0.00	0.00	0.00
	Volume Eq Cylinder	99.98	0.02	0.00	0.00	0.00	0.00	0.00	0.00	0.00	0.00	0.00	0.00	0.00	0.00	0.00	0.00	0.00	0.00	0.00	0.00	0.00
	Perimeter	0.11	39.81	16.41	10.77	7.52	5.32	4.13	2.81	2.61	1.94	1.35	2.22	1.34	1.04	1.16	1.02	0.27	0.07	0.07	0.01	0.03
	Mean Chord	1.38	93.10	4.17	0.90	0.29	0.08	0.02	0.02	0.01	0.01	0.00	0.01	0.00	0.00	0.00	0.00	0.00	0.00	0.00	0.00	0.00
	Length	0.41	71.33	12.03	6.57	3.37	2.10	1.39	0.75	0.68	0.31	0.28	0.26	0.17	0.14	0.08	0.09	0.00	0.00	0.03	0.00	0.00
	Width	11.61	84.82	2.91	0.49	0.10	0.04	0.02	0.00	0.00	0.01	0.00	0.00	0.00	0.00	0.00	0.00	0.00	0.00	0.00	0.00	0.00
	Max Feret	0.40	70.91	14.35	6.83	3.25	1.72	0.98	0.58	0.34	0.13	0.21	0.16	0.07	0.02	0.03	0.02	0.01	0.00	0.00	0.00	0.00
	Min Feret	1.35	84.87	8.46	2.98	1.21	0.47	0.29	0.10	0.09	0.08	0.04	0.02	0.02	0.00	0.02	0.01	0.00	0.00	0.00	0.00	0.00
	Circularity	0.00	0.00	0.00	0.00	0.00	0.00	0.00	0.00	0.00	0.00	0.00	0.00	0.01	0.03	0.04	0.79	4.62	9.26	12.99	72.25	0.00
	Elongation	0.00	0.00	0.00	0.00	0.00	0.00	0.00	0.00	0.00	0.00	0.00	0.00	0.00	0.00	0.00	0.00	0.00	0.00	0.00	0.11	99.89
Nadarzyn IG 1 2602.1	Eq diameter	1.22	79.74	7.90	3.93	2.25	1.64	0.91	0.72	0.54	0.36	0.24	0.22	0.16	0.03	0.11	0.03	0.00	0.00	0.00	0.00	0.00
	Volume Eq Sphere	99.79	0.21	0.00	0.00	0.00	0.00	0.00	0.00	0.00	0.00	0.00	0.00	0.00	0.00	0.00	0.00	0.00	0.00	0.00	0.00	0.00
	Volume Eq Cylinder	99.92	0.08	0.00	0.00	0.00	0.00	0.00	0.00	0.00	0.00	0.00	0.00	0.00	0.00	0.00	0.00	0.00	0.00	0.00	0.00	0.00
	Perimeter	0.16	48.42	11.84	7.45	5.49	3.89	3.06	2.47	2.10	1.49	1.42	2.40	1.69	1.41	1.95	2.51	1.17	0.52	0.23	0.25	0.05
	Mean Chord	2.46	87.26	5.24	2.38	1.32	0.71	0.27	0.13	0.11	0.03	0.03	0.05	0.00	0.00	0.00	0.00	0.00	0.00	0.00	0.00	0.00
	Length	0.78	69.70	9.32	5.64	3.56	2.44	1.79	1.38	1.03	0.77	0.63	0.79	0.73	0.36	0.50	0.37	0.13	0.04	0.02	0.00	0.00
	Width	17.20	74.44	4.80	1.90	0.95	0.40	0.14	0.10	0.03	0.04	0.00	0.00	0.00	0.00	0.00	0.00	0.00	0.00	0.00	0.00	0.00
	Max Feret	0.78	69.47	11.05	6.05	3.57	2.28	1.72	1.24	0.83	0.52	0.67	0.76	0.45	0.20	0.20	0.16	0.05	0.00	0.00	0.00	0.00
	Min Feret	2.20	80.88	6.90	3.60	2.12	1.54	0.72	0.66	0.46	0.22	0.25	0.21	0.12	0.02	0.09	0.02	0.00	0.00	0.00	0.00	0.00
	Circularity	0.00	0.00	0.00	0.00	0.00	0.00	0.00	0.01	0.00	0.02	0.04	0.05	0.10	0.11	0.42	2.26	6.22	9.78	11.83	69.14	0.00
	Elongation	0.00	0.00	0.00	0.00	0.00	0.00	0.00	0.00	0.00	0.00	0.00	0.00	0.00	0.00	0.00	0.00	0.00	0.00	0.00	0.16	99.84
Warka IG 1 2069.2	Eq diameter	0.71	78.25	11.89	4.98	2.21	0.95	0.52	0.25	0.09	0.08	0.03	0.06	0.00	0.00	0.00	0.00	0.00	0.00	0.00	0.00	0.00
	Volume Eq Sphere	100.00	0.00	0.00	0.00	0.00	0.00	0.00	0.00	0.00	0.00	0.00	0.00	0.00	0.00	0.00	0.00	0.00	0.00	0.00	0.00	0.00
	Volume Eq Cylinder	100.00	0.00	0.00	0.00	0.00	0.00	0.00	0.00	0.00	0.00	0.00	0.00	0.00	0.00	0.00	0.00	0.00	0.00	0.00	0.00	0.00
	Perimeter	0.07	40.00	13.60	9.32	6.77	5.21	4.11	3.59	2.92	2.24	1.95	2.94	1.94	1.45	1.71	1.64	0.37	0.12	0.03	0.02	0.00
	Mean Chord	1.49	90.48	6.01	1.43	0.42	0.12	0.05	0.01	0.00	0.00	0.00	0.00	0.00	0.00	0.00	0.00	0.00	0.00	0.00	0.00	0.00
	Length	0.42	66.31	12.74	7.37	4.37	2.60	1.97	1.21	0.84	0.71	0.46	0.41	0.20	0.17	0.13	0.07	0.01	0.00	0.00	0.00	0.00

Table 2 cont.

1	2	3	4	5	6	7	8	9	10	11	12	13	14	15	16	17	18	19	20	21	22	23
cd. Warka IG 1 2069.2	Width	12.51	82.20	4.23	0.76	0.26	0.04	0.01	0.00	0.00	0.00	0.00	0.00	0.00	0.00	0.00	0.00	0.00	0.00	0.00	0.00	0.00
	Max Feret	0.42	67.25	14.63	7.88	4.30	2.44	1.28	0.68	0.43	0.29	0.14	0.15	0.08	0.04	0.01	0.00	0.00	0.00	0.00	0.00	0.00
	Min Feret	1.43	79.59	11.04	4.47	1.87	0.80	0.41	0.14	0.09	0.08	0.03	0.03	0.01	0.00	0.00	0.00	0.00	0.00	0.00	0.00	0.00
	Circularity	0.00	0.00	0.00	0.00	0.00	0.00	0.00	0.00	0.00	0.01	0.00	0.02	0.02	0.02	0.08	1.45	5.99	11.23	12.99	68.20	0.00
	Elongation	0.00	0.00	0.00	0.00	0.00	0.00	0.00	0.00	0.00	0.00	0.00	0.00	0.00	0.00	0.00	0.00	0.00	0.00	0.00	0.07	99.93
Warka IG 1 2259.1	Eq diameter	1.15	91.95	5.77	0.93	0.19	0.01	0.00	0.00	0.00	0.00	0.00	0.00	0.00	0.00	0.00	0.00	0.00	0.00	0.00	0.00	0.00
	Volume Eq Sphere	100.00	0.00	0.00	0.00	0.00	0.00	0.00	0.00	0.00	0.00	0.00	0.00	0.00	0.00	0.00	0.00	0.00	0.00	0.00	0.00	0.00
	Volume Eq Cylinder	100.00	0.00	0.00	0.00	0.00	0.00	0.00	0.00	0.00	0.00	0.00	0.00	0.00	0.00	0.00	0.00	0.00	0.00	0.00	0.00	0.00
	Perimeter	0.13	48.54	17.81	10.22	6.83	4.76	3.35	2.41	1.60	1.05	0.92	1.12	0.54	0.37	0.26	0.08	0.00	0.00	0.00	0.00	0.00
	Mean Chord	1.97	97.43	0.60	0.00	0.00	0.00	0.00	0.00	0.00	0.00	0.00	0.00	0.00	0.00	0.00	0.00	0.00	0.00	0.00	0.00	0.00
	Length	0.72	79.12	10.82	4.77	2.23	1.15	0.56	0.34	0.15	0.07	0.04	0.02	0.01	0.00	0.00	0.00	0.00	0.00	0.00	0.00	0.00
	Width	14.34	85.53	0.13	0.00	0.00	0.00	0.00	0.00	0.00	0.00	0.00	0.00	0.00	0.00	0.00	0.00	0.00	0.00	0.00	0.00	0.00
	Max Feret	0.72	80.67	12.56	4.17	1.38	0.36	0.11	0.03	0.00	0.00	0.00	0.00	0.00	0.00	0.00	0.00	0.00	0.00	0.00	0.00	0.00
	Min Feret	1.93	92.02	4.98	0.90	0.14	0.02	0.00	0.00	0.00	0.00	0.00	0.00	0.00	0.00	0.00	0.00	0.00	0.00	0.00	0.00	0.00
	Circularity	0.00	0.00	0.00	0.00	0.00	0.00	0.00	0.00	0.00	0.00	0.00	0.01	0.01	0.03	0.11	1.84	6.21	9.44	10.98	71.38	0.00
	Elongation	0.00	0.00	0.00	0.00	0.00	0.00	0.00	0.00	0.00	0.00	0.00	0.00	0.00	0.00	0.00	0.00	0.00	0.00	0.00	0.13	99.87
Wilga IG 1 1912.8	Eq diameter	1.43	91.48	5.36	1.19	0.31	0.10	0.05	0.04	0.02	0.00	0.01	0.00	0.00	0.00	0.00	0.00	0.00	0.00	0.00	0.00	0.00
	Volume Eq Sphere	100.00	0.00	0.00	0.00	0.00	0.00	0.00	0.00	0.00	0.00	0.00	0.00	0.00	0.00	0.00	0.00	0.00	0.00	0.00	0.00	0.00
	Volume Eq Cylinder	100.00	0.00	0.00	0.00	0.00	0.00	0.00	0.00	0.00	0.00	0.00	0.00	0.00	0.00	0.00	0.00	0.00	0.00	0.00	0.00	0.00
	Perimeter	0.20	52.71	16.09	8.81	5.85	4.13	3.08	2.30	1.63	1.20	1.00	1.18	0.65	0.43	0.39	0.26	0.07	0.02	0.01	0.00	0.00
	Mean Chord	2.52	96.37	0.94	0.11	0.05	0.02	0.00	0.00	0.00	0.00	0.00	0.00	0.00	0.00	0.00	0.00	0.00	0.00	0.00	0.00	0.00
	Length	0.92	78.88	9.79	4.96	2.55	1.23	0.66	0.37	0.23	0.14	0.10	0.07	0.06	0.04	0.01	0.02	0.00	0.00	0.00	0.00	0.00
	Width	17.80	81.62	0.50	0.07	0.02	0.00	0.00	0.00	0.00	0.00	0.00	0.00	0.00	0.00	0.00	0.00	0.00	0.00	0.00	0.00	0.00
	Max Feret	0.91	80.91	11.59	4.05	1.55	0.57	0.15	0.12	0.07	0.04	0.02	0.01	0.01	0.00	0.00	0.00	0.00	0.00	0.00	0.00	0.00
	Min Feret	2.35	91.44	4.66	1.07	0.27	0.11	0.04	0.05	0.01	0.00	0.01	0.00	0.00	0.00	0.00	0.00	0.00	0.00	0.00	0.00	0.00
	Circularity	0.00	0.00	0.00	0.00	0.00	0.00	0.00	0.00	0.01	0.01	0.02	0.02	0.03	0.07	0.32	3.31	7.32	9.80	9.83	69.27	0.00
	Elongation	0.00	0.00	0.00	0.00	0.00	0.00	0.00	0.00	0.00	0.00	0.00	0.00	0.00	0.00	0.00	0.00	0.00	0.00	0.00	0.20	99.80

Tabela 3

Effective porosity in selected sandstone samples

Wyniki porowatości efektywnej w wybranych próbkach piaskowców

Borehole	Depth [m]	Effective porosity [%]
Białobrzegi IG 1	2185.0	16.12
	2219.5	1.71
	2254.6	10.60
	2268.6	5.72
	2388.4	5.18
Maciejowice IG 1	1738.5	25.60
	1740.0	27.70
	1741.5	29.50
	1745.5	30.90
	1746.5	22.30
	1750.0	28.30
	1753.0	26.10
	1754.0	29.90
	1756.0	22.80
	1756.5	26.20
	1760.7	21.40
	1761.7	16.60
	1764.0	23.00
Nadarzyn IG 1	2550.5	14.74
	2553.1	4.28
	2556.3	13.56
	2601.2	20.30
	2607.4	16.79
	2612.5	20.70
	2659.0	21.50
	2664.5	8.86
	2719.2	1.72
	2724.8	19.52
	2730.6	8.07
	2779.8	1.60
	2782.7	4.35
Warka IG 1	2070.0	2.00
	2107.0	24.70
	2139.0	25.82
	2172.0	23.20
	2206.0	23.15
	2255.0	4.18
	2256.3	4.46
Wilga IG 1	1897.0	18.10
	1902.0	9.84
	1907.0	28.40
	1909.0	27.80
	1913.8	27.10
	1914.8	26.30
	1919.0	28.80
	1923.0	30.30

REFERENCES

ALEKSANDROWSKI P., 2017 – Struktury mezozoiczne (staroalpejskie). *In*: Atlas geologiczny Polski (eds. J. Nawrocki, A. Becker): 42. Państw. Inst. Geol. – PIB, Warszawa.

BACHMANN G.H., GELUK M.C., WARRINGTON G., BECKER-ROMAN A., BEUTLER G., HAGDORN H., HOUNSLOW M.W., NITSCH E., RÖHLING H.-G., SIMON T., SZULC A., 2010 – Triassic. *In*: Petroleum Geological Atlas of the Southern Permian Basin Area (eds. J.C. Doornenbal, A.G. Stevenson): 149–173. EAGE Publications b.v., Houten.

BECKER A., 2019a – Pstry piaskowiec i kajper – litologia, stratygrafia, zarys przebiegu sedymentacji. *In*: Bodzanów IG 1 (ed. K. Leszczyński). *Profile Głęb. Otw. Wiert. Państw. Inst. Geol*. (in preparation).

BECKER A., 2019b – Wykształcenie litologiczne, stratygrafia i zarys przebiegu sedymentacji pstrego piaskowca. *In*: Wilga IG 1 (eds. M.I. Waksmundzka, K. Wójcik). *Profile Głęb. Otw. Wiert. Państw. Inst. Geol*. (in preparation).

CBDG, 2008 – Centralna Baza Danych Geologicznych. Litostratygrafia, Chronostratygrafia, Litologia, weryfikacja 2008. Internet: http://otworywiertnicze.pgi.gov.pl (access: 14.02.2019).

CHADWICK A., ARTS R., BERNSTONE C., MAY F., THIBEAU S., ZWEIGEL P. (eds.), 2006 – Best Practice for the Storage of CO_2 in Saline Aquifers, Observations and guidelines from the SACS and CO2STORE projects. Raport projektu CO2STORE. Internet: www.co2store.org (access: 14.02.2019).

DYRKA I., 2018 – Analiza tempa depozycji oraz modelowanie historii termicznej i warunków pogrzebania. *In*: Polik IG 1 (eds. T. Podhalańska, M. Sikorska-Jaworowska). *Profile Głęb. Otw. Wiert. Państw. Inst. Geol*., **150**: 137–140.

FELDMAN-OLSZEWSKA A., ADAMCZAK-BIAŁY T., BECKER A., 2012 – Charakterystyka poziomów zbiornikowych i uszczelniających formacji jury i triasu północnego Mazowsza pod kątem geologicznego składowania CO_2 na podstawie danych z głębokich otworów wiertniczych. *Biul. Państw. Inst. Geol*., **448**: 27–46.

KOZŁOWSKA, A., KUBERSKA M., 2006 – Zastosowanie metody komputerowego przetwarzania i analizy obrazu w mikroskopowej analizie skał. *Prz. Geol*., **54**, 8: 671–673.

KUBERSKA M., 1997 – Trias dolny. Charakterystyka petrograficzna. *In*: Epikontynentalny perm i mezozoik w Polsce. *Pr. Państw. Inst. Geol*., **153**: 117–121.

KUBERSKA M., 1999 – Trias dolny – pstry piaskowiec. *In*: Diageneza osadów permu górnego i mezozoiku Kujaw. *Pr. Państw. Inst. Geol*., **167**: 22–35.

LEŚNIAK G., 1999 – Zastosowanie komputerowej analizy obrazu w badaniach petrofizycznych. *Prz. Geol*., **47**, 7: 644–651.

MAREK S., 1983 – Budowa geologiczna niecki warszawskiej (płockiej) i jej podłoża. *Pr. Inst. Geol*., **103**.

MIGASZEWSKI Z., NARKIEWICZ M., 1983 – Identyfikacja pospolitych minerałów węglanowych przy użyciu wskaźników barwiących. *Prz. Geol*., **4**: 258–261.

NARKIEWICZ M., DADLEZ R., 2008 – Geologiczna regionalizacja Polski – zasady ogólne i schemat podziału w planie podkenozoicznym i podpermskim. *Prz. Geol*., **56**, 5: 391–397.

PETTIJOHN F.J., POTTER P.D., SIEVER R., 1972 – Sand and sandstone. Springer Verlag, Berlin.

PLEWA M., PLEWA S., 1992 – Petrofizyka. Wydaw. Geol., Warszawa.

SZYPERKO-ŚLIWCZYŃSKA A., 1980 – Trias dolny. Warka IG 1. *In*: Profile stratygraficzne otworów wiertniczych niecki warszawskiej (płockiej) (otwory głębsze niż 500 m) (ed. J. Smolicz). Załącznik do monografii pt. „Budowa geo-

logiczna Niecki Warszawskiej (Płockiej) i jej podłoża", praca zbiorowa, pod red. S. Marka. Inst. Geol., Warszawa.

SZYPERKO-TELLER A., SENKOWICZOWA H., KUBERSKA M., 1997 – Trias dolny (pstry piaskowiec). *In*: Epikontynentalny perm i mezozoik w Polsce (eds. S. Marek, M. Pajchlowa). *Pr. Państw. Inst. Geol*., **143**: 83–132.

WÓJCICKI A., 2013 – Rozpoznanie formacji i struktur do bezpiecznego geologicznego składowania CO_2 wraz z ich programem monitorowania. Raport końcowy. Internet: http://sklado-wanie.pgi.gov.pl (access: 14.02.2019).

WÓJCICKI A, KIERSNOWSKI H., DYRKA I., ADAMCZAK-BIAŁY T., BECKER A., GŁUSZYŃSKI A., JANAS M., KOZŁOWSKA A., KRZEMIŃSKI L., KUBERSKA M., PACZEŚNA J., PODHALAŃSKA T., ROMAN M., SKOWROŃSKI L., WAKSMUNDZKA M.I., 2014 – Prognostyczne zasoby gazu ziemnego w wybranych zwięzłych skałach zbiornikowych Polski. Państw. Inst. Geol. – PIB, Warszawa.

ŻELAŹNIEWICZ A., ALEKSANDROWSKI P., BUŁA Z., KARNKOWSKI P. H., KONON A., OSZCZYPKO N., ŚLĄCZKA A., ŻABA J., ŻYTKO K., 2011 – Regionalizacja tektoniczna Polski. Komitet Nauk Geologicznych PAN, Wrocław.

STRESZCZENIE

Charakterystykę przestrzeni porowej piaskowców triasu przeprowadzono na próbkach pochodzących z siedmiu otworów wiertniczych usytuowanych w okolicach Warszawy (fig. 1). Sukcesję triasu dolnego w tym rejonie tworzą głównie skały iłowcowo-mułowcowe, masywne lub laminowane z przewarstwieniami piaskowców (fig. 2). Wyróżniono tu pięć poziomów zdominowanych przez piaskowce, które poddano analizie właściwości kolektorskich. Piaskowce, reprezentujące arenity, rzadziej waki kwarcowe i subarkozowe, sporadycznie sublityczne, charakteryzują się strukturą psamitową, miejscami psamitowo-aleurytową. Są słabo zwięzłe i słabo wysortowane. Głównymi składnikami materiału detrytycznego są ziarna kwarcu monokrystalicznego, skalenie potasowe, rzadziej plagioklazy oraz litoklasty pochodzenia magmowego i osadowego. Materiał detrytyczny jest scementowany spoiwem typu matriks (mieszanina minerałów ilastych, związków żelaza i mułku), węglanami (dolomit, kalcyt), miejscami kwarcem autigenicznycm, kaolinitem lub chlorytami (fig. 3). Komputerowa analiza obrazu, zastosowana jako jedna z metod badania przestrzeni porowej wybranych próbek (tab. 1, 2), pozwoliła na określenie ich porowatości – od 2,30 do 16,33% obj., a długość i szerokość 90% porów zawiera się w przedziale od 0,01 do 0,04 mm. Wyniki porowatości efektywnej zaczerpnięte z dokumentacji wynikowych badanych otworów wiertniczych zamieszczono w tabeli 3. Na kształtowanie właściwości petrofizycznych badanych piaskowców miały wpływ: kompakcja mechaniczna, cementacja, procesy rozpuszczania i przeobrażania diagenetycznego (fig. 4). Nasilenie kompakcji mechanicznej było niezbyt duże. Znacznie bardziej uszczelniająco działała cementacja, szczególnie węglanami. Kaolinit, tworząc formy książeczkowe w przestrzeniach porowych, ograniczał zdolności filtracyjne skał, w przeciwieństwie do kaolinitu blokowego. Chloryty, w zależności od sposobu wykształcenia, mogły ograniczać przepuszczalność w osadzie, ale w niewielkim stopniu z uwagi na niską zdolność adsorpcji płynów.

Obserwacje mikroskopowe pozwoliły stwierdzić, że przestrzeń porowa w badanych próbkach jest zdominowana przez makropory i chaotycznie wykształcona. Piaskowce triasu dolnego w rejonie Warszawy mają właściwości kolektorskie, które tylko wybiórczo i punktowo spełniają petrofizyczne kryteria przydatności składowiskowej w kontekście sekwestracji dwutlenku węgla.